Development 133, 2639-2648 (2006) doi:10.1242/dev.02429

The *brain tumor* gene negatively regulates neural progenitor cell proliferation in the larval central brain of *Drosophila*

Bruno Bello, Heinrich Reichert and Frank Hirth*

Brain development in *Drosophila* is characterized by two neurogenic periods, one during embryogenesis and a second during larval life. Although much is known about embryonic neurogenesis, little is known about the genetic control of postembryonic brain development. Here we use mosaic analysis with a repressible cell marker (MARCM) to study the role of the *brain tumor* (*brat*) gene in neural proliferation control and tumour suppression in postembryonic brain development of *Drosophila*. Our findings indicate that overproliferation in *brat* mutants is due to loss of proliferation control in the larval central brain and not in the optic lobe. Clonal analysis indicates that the *brat* mutation affects cell proliferation in a cell-autonomous manner and cell cycle marker expression shows that cells of *brat* mutant clones show uncontrolled proliferation, which persists into adulthood. Analysis of the expression of molecular markers, which characterize cell types in wild-type neural lineages, indicates that *brat* mutant clones comprise an excessive number of cells, which have molecular features of undifferentiated progenitor cells that lack nuclear Prospero (Pros). *pros* mutant clones phenocopy *brat* mutant clones in the larval central brain, and targeted expression of wild-type *pros* in *brat* mutant clones promotes cell cycle exit and differentiation of *brat* mutant cells, thereby abrogating brain tumour formation. Taken together, our results provide evidence that the tumour suppressor *brat* negatively regulates cell proliferation during larval central brain development of *Drosophila*, and suggest that Prospero acts as a key downstream effector of *brat* in cell fate specification and proliferation control.

KEY WORDS: *Drosophila*, Brain tumor, Prospero, Stem cell, Progenitor cell, Proliferation, Tumour

INTRODUCTION

In *Drosophila*, as in other holometabolic insects, neural stem cells called neuroblasts proliferate during two neurogenic periods (for a review, see Campos-Ortega and Hartenstein, 1997). In the embryonic neurogenic period, individual neuroblasts delaminate in a stereotyped pattern from the neuroectoderm and divide repeatedly and asymmetrically to generate a new neuroblast and a smaller daughter cell, called a ganglion mother cell (GMC) (Campos-Ortega, 1997; Edenfeld et al., 2002; Skeath and Thor, 2003; Technau et al., 2006). Each GMC is a transient intermediate progenitor cell that generally divides once to produce two lineage-specific postmitotic ganglion cells (GCs), which subsequently initiate their differentiation processes. Towards the end of embryogenesis, most neuroblasts stop proliferating and enter a period of quiescence. During the second, larval neurogenic period, most neuroblasts resume proliferation and generate the majority of the cells that comprise the central brain and ventral ganglia of the adult (White and Kankel, 1978; Truman and Bate, 1988; Prokop and Technau, 1991; Ito and Hotta, 1992; Truman et al., 2004).

In contrast to embryonic neurogenesis, less is currently known about the genetic systems which control and limit the activity of neural progenitor cells during postembryonic development, notably in the developing brain, where over 90% of the neurons in the adult central nervous system are generated. A candidate gene for proliferation control in the fly brain is the tumour-suppressor gene *brain tumor* (*brat*) which encodes a member of the conserved NHL family of proteins that regulate growth and differentiation in a variety of organisms (Arama et al., 2000). Recessive mutations in *brat* lead to neoplastic overgrowth, characterized by a dramatic enlargement of the larval brain hemispheres and the ability of pieces of brain tissue to metastasize and form secondary tumours when injected into the abdomen of a wild-type host fly (Kurzik-Dumke et al., 1992; Woodhouse et al., 1998; Arama et al., 2000). However, the functional role of the *brat* gene in this process is not clear since the neural phenotype has not been characterized in detail and initial findings are contradictory. Thus, the brain overproliferation phenotype of *brat* mutants is thought to be primarily due to expansion of optic lobe neuroblasts (Kurzik-Dumke et al., 1992; Gateff et al., 1993), yet the major sites of *brat* expression in the CNS throughout development are not the optic lobes, but rather the central brain and ventral nerve cord (Arama et al., 2000). In addition to its involvement in brain development, the *brat* gene acts in translational repression during early embryogenesis (Sonoda and Wharton, 2001) and negatively regulates cell growth and ribosomal RNA synthesis in imaginal discs (Frank et al., 2002); whether *brat* acts by similar molecular mechanisms in the brain is not known.

In this report, we use molecular markers and mosaic analysis to study the role of *brat* in neural proliferation control and tumour suppression in the *Drosophila* brain. Our findings indicate that *brat* mutation leads to loss of proliferation control in the central brain. Mosaic analysis with a repressible cell marker (MARCM) analysis demonstrates a larval requirement for *brat* since induction of mutant clones in the first larval instar is sufficient to cause massive overproliferation in the central brain that continues into adulthood. Molecular analysis of *brat* MARCM mutant clones demonstrates that loss of *brat* function leads to loss of nuclear Prospero (Pros) expression. Both *brat* and *pros* mutant MARCM clones comprise supernumerary cells, which do not express neuron-specific markers

Biozentrum, University of Basel, Klingelbergstrasse 50, CH-4056 Basel, Switzerland.

*Author for correspondence (e-mail: frank.hirth@unibas.ch)

Accepted 5 May 2006

such as Embryonic lethal abnormal vision (Elav). By contrast, the vast majority of cells in mutant clones strongly express molecular markers and cell cycle control genes which characterize neural progenitor cells of the wild-type postembryonic brain. Detailed clonal analysis indicates that loss of *brat* function, and loss of *pros* function, cell-autonomously affect the differentiation of ganglion cells. Targeted expression of wild-type *brat* or wild-type *pros* in *brat* mutant clones restores cell cycle exit and differentiation of *brat* mutant cells, which in turn abrogates central brain tumour formation. Taken together, our results demonstrate that the tumour suppressor *brat* negatively regulates cell proliferation during larval central brain development of *Drosophila* and identify *prospero* as a downstream effector of *brat* in cell fate specification and proliferation control.

MATERIALS AND METHODS

Drosophila stocks and mosaic analysis

Most fly stocks carrying transgenes and recombinant chromosomes were obtained from the Bloomington Stock Center and their detailed description can be found at FlyBase (http://flybase.bio.indiana.edu). Other stocks were kindly provided by colleagues: $GAL4^{NP3262}$ (GETDB database, http://flymap.lab), *FRT40A,* $brat^{11}$ (Frank et al., 2002) (a gift from D. Frank); *FRT82B,* $pros^{17}$ (Reddy and Rodrigues, 1999) (a gift from V. Rodrigues); *UAS-*$brat^{FL1B}$ (Sonoda and Wharton, 2001) (a gift from R. Wharton); *UAS-*$pros^{L(wt)9D}$ (a gift from C. Doe). The following recombinant chromosomes other than described in Bello et al. (Bello et al., 2003), were generated for this study: $brat^{11}$, $GAL4^{NP3262}$*; FRT40A, UAS-mCD8::*GFP^{LL5}*, UAS-nlslacZ*^{20b}*; FRT40A, UAS-mCD8::*GFP^{LL5}*;* $brat^{11}$*, UAS-mCD8::*GFP^{LL5}*, UAS-nlslacZ*^{20b}. GFP labelling of wild-type and zygotic brat mutant larval nervous systems was achieved by crossing $brat^{11}$, $GAL4^{NP3261}$*/CyO, actGFP*^{JMR1} to *FRT40A; UAS-mCD8::*GFP^{LL6}*, UAS-nlslacZ*^{J312} or *FRT40A,* $brat^{11}$*/CyO, actGFP*^{JMR1}*; UAS-mCD8::*GFP^{LL6}*, UAS-nlslacZ*^{J312}. Heterozygous wild-type and homozygous *brat* mutant larvae lacking *CyO, actGFP*^{JMR1} were selected under the fluorescence microscope. The detailed MARCM genotypes indicated in the figure legends were obtained from various stocks assembled using standard genetics.

For MARCM experiments, embryos of the appropriate genotype were collected on yeasted grape juice-agar plates over a 4- to 6-hour time window and raised at 25°C for 24-28 hours before heat shock treatment. Heat-shock induction of FLP in the newly hatched larvae was performed by immersing the plates at 37°C in a water bath for 60 minutes. Larvae were then collected and plated at low density on standard cornmeal/yeast/agar medium supplemented with live yeast. GFP-labelled MARCM clones were examined in mid (66-72 hours) to late (96-120 hours) third instar larval central nervous systems (CNSs).

Immunocytochemistry and image acquisition

Larval tissues were fixed and immunostained as previously described (Bello et al., 2003). To generate a neural progenitor cell-specific anti-grainy head (Grh) antibody, a synthetic peptide covering 19AA of Grh [aa 798-816 of the O-isoform (Uv et al., 1997)] was used for immunization of rabbits (carried out by Neosystems). Polyclonal rabbit anti-Grh 711 was used at a 1:200 dilution. Other primary antibodies used were: rat anti-Brat (Sonoda and Wharton, 2001) 1:200; rabbit anti-β-galactosidase (β-gal; Cappel) 1:7000; mouse anti-β-gal (Promega) 1:1000; rabbit anti-PH3 (Upstate Biotechnology) 1:400; mouse anti-Mira [mAb81 (Matsuzaki et al., 1992); a gift from P. Overton] 1:50; mouse anti-Pros (mAbMR1A, Developmental Studies Hybridoma Bank, DSHB, Iowa University) 1:5; mouse anti-cyclin B (CycB) (mAbF2F4, DSHB) 1:10, mouse anti-CycE (mAb8B10; a gift from H. Richardson) 1:50; rat anti-Elav (mAb7E8A10, DSHB) 1:30; and mouse anti-Grh (BF1; a gift from S. Bray) 1:3. All fluorescent images were captured using a Leica TCS SP scanning confocal microscope. Optical sections ranged from 0.5 to 2 μm, recorded in line average mode with picture size of 512×512 pixels. Captured images from optical sections were arranged and processed using IMARIS (Bitplane) or ImageJ software. Figures were arranged and labelled using Adobe Photoshop.

RESULTS

brat mutation perturbs development of the larval central brain

Inactivation of *brat* alleles in homozygous individuals results in the production of tumour-like neoplasm in the larval brain (Arama et al., 2000). The overgrowth of brain hemispheres is gradual during larval development and becomes prominent in whole mounts of late third larval instars (Fig. 1A,B). At earlier larval stages, brain hemispheres in *brat* mutants still have the same overall size as in wild type; in both cases, the larval brain hemispheres are characterized by a central brain region and laterally located developing optic lobes (Fig. 1C,D). Examination of cell morphology in the wild-type central brain reveals a limited number of large cells, which are the postembryonic neuroblasts, associated with smaller cells, which are their progeny (Fig. 1E). By contrast, the *brat* mutant central brain is characterized by dense cellular masses of numerous small and pleiomorphic cells in addition to a limited number of large cells (Fig. 1F).

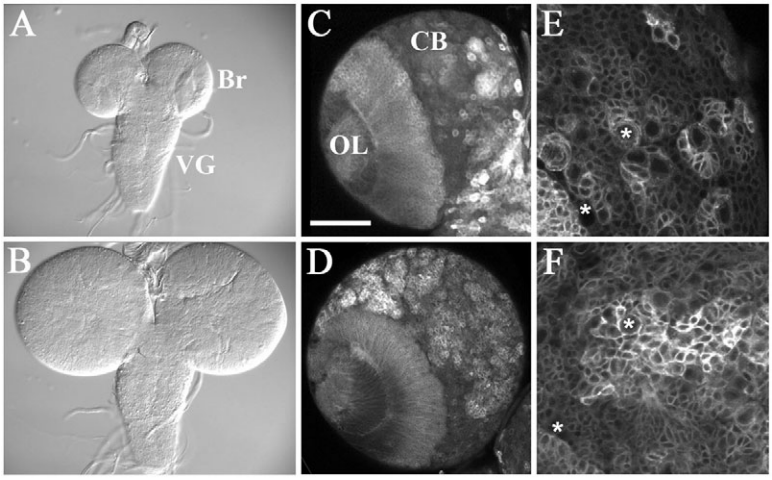

Fig. 1. *brat* mutation perturbs development of the larval central brain. $GAL4^{NP3262}$ driven *UAS-mCD8::GFP* expression in heterozygous (**A**,**C**,**E**) and homozygous (**B**,**D**,**F**) zygotic *brat* mutant larval CNS reveals all cell membranes of secondary lineages in central brain (CB) and optic lobe (OL). (A,B) In late third instar *brat* mutant larvae, brain hemispheres (Br) are markedly enlarged and characterized by cellular overgrowth whereas ventral ganglia (VG) appear normal (compare B with A). (C,D) In early to mid third instar larvae, brain hemispheres of *brat* mutants appear of same size as heterozygous brain hemispheres when viewed as whole mounts (D, compare with C). The cellular architecture of optic lobes is unaltered but is pushed aside by overgrowth of the central brain area that displays abnormal cells types. (E) Higher magnification of heterozygous central brain area in C reveals a regular pattern of large superficial neuroblasts (asterisks), in association with smaller numerous progeny cells. (F) By contrast, higher magnification of central brain area in D reveals that *brat* mutant brain tissue is characterized by dense cellular masses of numerous small, pleiomorphic cells in addition to larger cells, presumably neuroblasts (asterisks). Scale bar, 70 μm. Genotypes: (A,C,E) $brat^{11}$, $GAL4^{NP3262}$*/FRT40A; UAS-mCD8::*GFP^{LL6}*, UAS-nlslacZ*^{J312}/+. (B,D,F) $brat^{11}$, $GAL4^{NP3262}$*/FRT40A,* $brat^{11}$*; UAS-mCD8::*GFP^{LL6}*, UAS-nlslacZ*^{J312}/+.

brat mutation affects postembryonic cell proliferation in a cell-autonomous manner

In order to gain insights into the origin and genetic mechanisms of tumour formation caused by loss of *brat* function, we used MARCM clonal analysis to label individual *brat* mutant neural lineages in a wild-type heterozygous background (Lee and Luo, 1999; Lee and Luo, 2001). Positively marked somatic clones mutant for $brat^{11}$, a strong loss-of-function allele of *brat*, were generated and examined 4 days later in late third instar larvae. Wild-type clones were induced in parallel as control, hence for each genotype (wild type and *brat*) we examined more than 300 specimens carrying 5-20 clones in each brain hemispheres. Our analysis indicated that *brat* mutant clones in the larval optic lobes are indistinguishable from wild-type clones. By contrast, *brat* mutant clones in the larval central brain populated large areas of the brain hemispheres (Fig. 2C), as compared to wild-type central brain clones (Fig. 2A). Whereas wild-type clones are composed of 50-100 cells in average (n>100), the majority of late third instar *brat* mutant clones (n>100) were up to ten times larger than control clones. Thus, less than 20% of *brat* mutant clones comprised <100 cells, whereas more than 80% of the clones comprised 200-1000 cells. Examination of mutant clones in early third instar larvae revealed clearly distinguishable and separated *brat* mutant clones (not shown), whereas in late third instars, we frequently observed hemispheres within which the central brain was almost entirely labelled with GFP (Fig. 2C). This suggested that multiple *brat* mutant clones had already merged into an indistinguishable labelled cell mass overgrowing the whole central brain.

By contrast to the central brain area, *brat* mutant clones in larval ventral ganglia appeared normal, both in size and shape, when compared to wild-type control clones (Fig. 2B,D). These data suggest that *brat* affects cell proliferation in a cell-autonomous manner specifically in the larval central brain. We, therefore, wondered whether we could identify, more precisely, the central brain area within which proliferation defects in *brat* mutant clones occur. Our clone induction protocol revealed that increase in size of mutant clones initiated frequently in the dorsal central brain, however, due to the lack of region-specific anatomical markers, we could not allocate this region in more detail. Nevertheless, we could exclude the possibility that the affected central brain area covers the mushroom body neuroblasts. In the wild-type central brain, mushroom body neuroblasts are exceptional with regard to frequency and temporal window of proliferation (Truman and Bate, 1988). Yet, *brat* mutant clones of mushroom body neuroblast lineages did not result in enlarged clones (data not shown).

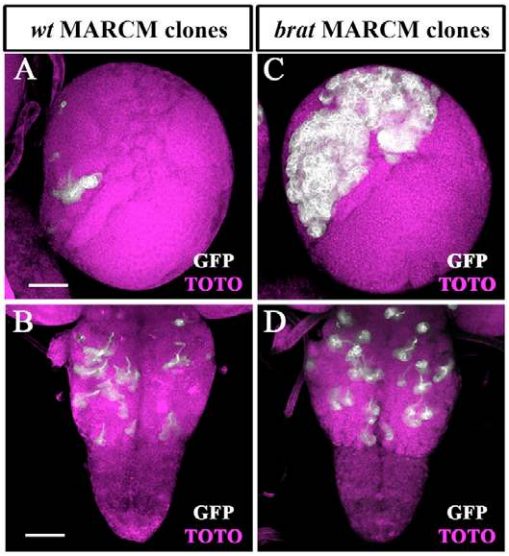

Fig. 2. The *brat* mutation affects larval central brain proliferation in a cell-autonomous manner. Wild-type (**A**,**B**) and $brat^{11}$ (**C**,**D**) MARCM clones labelled with CD8::GFP in third instar larval brain hemispheres (A,C) and ventral ganglia (B,D), counterstained with the DNA dye TOTO-3. When induced at low frequency in newly hatched larvae, wild-type clones contain progeny of a single neuroblast occupying a small area of third instar larval brain (single clone shown in A). Similar heat shock conditions generate $brat^{11}$ mutant clones of large size, which appear difficult to resolve as single neuroblast lineages (two or more merged clones are shown in C). In ventral ganglia, $brat^{11}$ mutant clones (D) are recovered at similar frequency as in wild-type clones (B) and appear indistinguishable in size and shape. Scale bars, 50 μm. Genotypes: (A,B) *hsFLP/+; FRT40A, UAS-mCD8::GFP^{LL5}, UAS-nlslacZ^{20b}/FRT40A, tubP-GAL80^{LL10}; tubP-GAL4^{LL7}/+*; (C,D) *hsFLP/+; FRT40A, brat^{11}, UAS-mCD8::GFP^{LL5}, UAS-nlslacZ^{20b}/FRT40A, tubP-GAL80^{LL10}; tubP-GAL4^{LL7}/+*.

Proliferation in wild-type neural lineages of the larval central brain

To investigate the nature of the cells that overproliferate in *brat* mutant lineages, we first defined a set of molecular markers that enabled us to characterize the cell types in wild-type neural lineages. Wild-type MARCM clones examined in late third instar animals typically contain a single large neuroblast (~10 μm in size) associated with a discrete packet of smaller cells that corresponds to its entire progeny generated during larval development (Fig. 3A) (Bello et al., 2003). The latter population is mostly composed of immature adult-specific ganglion cells which extend neurites towards the inner neuropile. Neuronal extensions associate in a common bundle known as cell body fibre tract (CBT) (Fig. 3A).

Neuroblasts express the coiled-coiled protein Miranda (Mira) at the cell cortex (Ceron et al., 2001; Akong et al., 2002). Cortical Mira becomes polarized during mitosis forming a crescent that segregates into the budding GMC (Fig. 3C). The transcription factor Grainy head (Grh) also labels the large neuroblast (Fig. 3H). The mitotic profile of the neuroblast is revealed by expression of the cell cycle markers phosphorylated histone H3 (PH3) (Fig. 3B,D) and CycE (Fig. 3D,E). Careful inspection of mitosis using the nuclear localisation of PH3 and visualisation of centrosomes further indicates that CycE protein is detectable in neuroblasts throughout the cell cycle.

Although GMCs are not distinguishable morphologically from the surrounding postmitotic ganglion cells, their identification in close proximity to the parental neuroblast is defined in wild-type clones by expression of the cell cycle markers CycE (Fig. 3D,E) and/or PH3 (Fig. 3E-G), as well as nuclear Grh expression (Fig. 3H) (Cenci and Gould, 2005; Almeida and Bray, 2005) and association of Mira at the cellular cortex (Fig. 3F,I). Beside their difference in size, two molecular characteristics make it possible to distinguish neuroblasts and GMCs. First, expression of CycE is detectable in GMCs only at interphase (PH3-negative nucleus, Fig. 3D) but not during mitosis (PH3-positive nucleus, Fig. 3E). Second, localisation of Mira at the cellular cortex is never polarized during GMC mitosis (PH3-positive nucleus in Fig. 3F).

GMCs are also characterized by nuclear localization of Pros, which is clearly detectable by co-staining with PH3 (Fig. 3G) or Grh (Fig. 3H). In addition, nuclear Pros expression is also detectable in

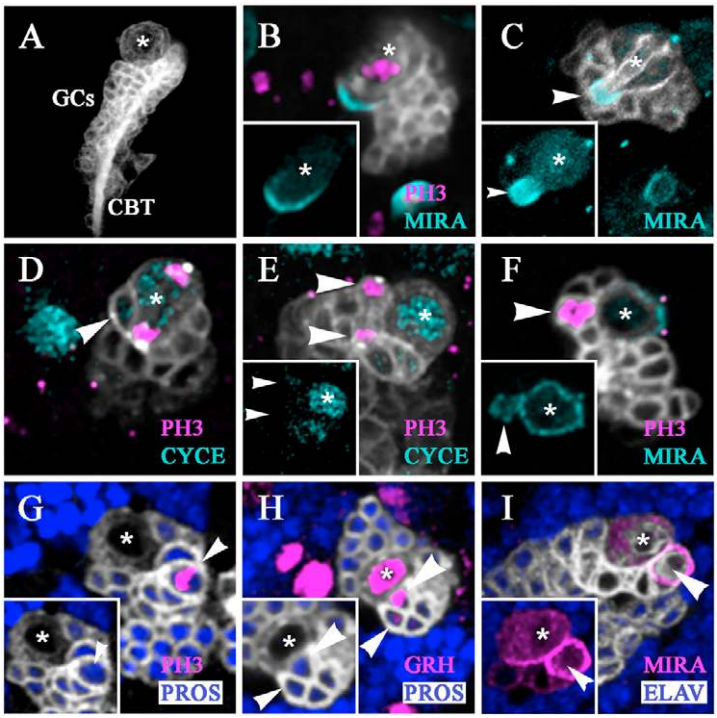

Fig. 3. Cell markers and proliferation of wild-type neural lineages in the larval central brain. Wild-type MARCM clones labelled with membrane-tethered CD8::GFP (A-I; white) and centrosomin-GFP for centrosomes (D,E; white dots). Neuroblasts are indicated by asterisks and closely associated GMCs by arrowheads. (**A**) GFP-labelling of an entire clone shows a single large neuroblast and its associated progeny of adult-specific neurons (ganglion cells; GCs) which send their neurite in a common bundle (cell body fibre tract; CBT). (**B-I**) Neuroblast and late born cells are shown, immunostained as indicated in each panel. Mitosis, detected by PH3 immunostaining, is always restricted to neuroblasts (B: metaphase; D: telophase) and GMCs (E: anaphase/telophase; F,G: prophase/metaphase). CycE is detectable in neuroblast from interphase (E) to telophase (D) and in terminally dividing GMCs at interphase (D), but not during terminal division (E, inset shows CycE only). Mira is polarised at the neuroblast cortex during mitosis forming a crescent at metaphase (B) that segregates in budding GMC at telophase (C). Uniform cortical Mira is detected in neuroblasts at interphase (F,I) or in GMCs during mitosis (F, inset shows Mira only). Both neuroblasts and GMCs show Grh in their nuclei (H), whereas Pros is detectable in all nuclei of GMCs and GCs but not in the nucleus of neuroblasts (G,H, inset shows Pros staining only). Elav is expressed exclusively in nuclei of GCs that do not express Mira (I). Genotypes: (A-C,F-G) *hsFLP/+; FRT40A/ FRT40A, tubP-GAL80^{LL10}; UAS-mCD8::GFP^{LL6}, UAS-nlslacZ^{J312}/tubP-GAL4^{LL7}*. (D,E) *hsFLP/UAS-cnn::GFP; FRT40A, UAS-mCD8::GFP^{LL5}/FRT40A, tubP-GAL80^{LL10}; tubP-GAL4^{LL7}/+*.

postmitotic ganglion cells (Fig. 3G,H), which also express the neuronal marker Elav (Fig. 3I). These data show that in wild-type neural lineages of the larval central brain, only neuroblasts and GMCs are actively engaged in the cell cycle, and that each cell type can be unambiguously identified by a unique combination of markers (Table 1).

brat mutant clones comprise an excessive number of neural progenitor cells

We next used these molecular markers to characterize *brat* mutant lineages in the central brain. Previous genome-wide transcript profiling of adult *brat^{k06028}* mutant brains had revealed high expression levels of cell cycle regulators (Loop et al., 2004). To determine whether the observed increase in cell number reflects changes in cell cycle regulation, we analyzed the distribution of cell cycle markers in *brat^{11}* clones using antibodies against CycE, CycB and PH3. In sharp contrast to wild-type neuroblast lineages, most *brat* mutant cells within a labelled mass of clones expressed CycE (Fig. 4A) and CycB (not shown) and a large number of cells appeared engaged in mitosis as indicated by PH3 staining of numerous nuclei (Fig. 4B,E).

With few exceptions, all mutant cells within the clones lacked immunoreactivity for nuclear Pros (Fig. 4C,C′) and nuclear Elav (Fig. 4D), unlike the surrounding heterozygous wild-type cells devoid of GFP labelling. Moreover, we never observed any cellular extensions comparable to axon fascicles, suggesting an invariable lack of axonal processes. Since MARCM clones allow unambiguous identification of neuronal processes in both, wild-type and various mutant lineages, due to stable GFP labelling (Lee and Luo, 1999; Lee and Luo, 2001), these data suggest that *brat* mutant cells are impaired in differentiation. In support of this notion, we observed that the vast majority of cells in *brat* mutant clones showed both nuclear Grh (Fig. 4C,C′) and cortical Mira (Fig. 4E). Close inspection of clones revealed that a few large cells scattered at the surface showed polarized Mira distribution in a cortical crescent. As in wild-type neuroblasts, this asymmetric distribution of Mira was always associated with PH3 immunoreactivity, suggesting the presence of several asymmetrically dividing neuroblasts because of the merger of individual GFP-labelled *brat* mutant clones (see also Fig. 2C). In contrast to these large cells displaying Mira in a cortical crescent, the majority of mutant cells showed uniform cortical distribution of Mira even during mitosis (Fig. 4E). These data indicate that *brat* mutant clones comprise an excessive number of neural progenitor cells that are unable to exit the cell cycle but continue to proliferate.

brat mutant cells in the central brain continue to proliferate into adulthood

Previous studies have shown that cessation of proliferation in the developing *Drosophila* brain occurs during puparium formation and metamorphosis (Ito and Hotta, 1992). We, therefore,

Table 1. Neural lineage cell types in the larval central brain can be identified by a unique combination of markers

		Markers detected by immunostaining					
		Mira (cell cortex)				CycE	
Cell type	Grh nucl.	Interphase	Mitosis	Pros nucl.	Elav nucl.	Interphase	Mitosis
NB	+	Uniform	Asymm.	–	–	+	+
GMC	+	Uniform	Uniform	+	–	+	–
GC	–	–	n/a	+	+	–	–

NB, neuroblast; GMC, ganglion mother cell; GC, ganglion cell; +, Positive immunostaining; –, no immunostaining; nucl., nuclear localization; uniform, uniform cortical distribution; asymm., asymmetric cortical distribution; n/a, not applicable.

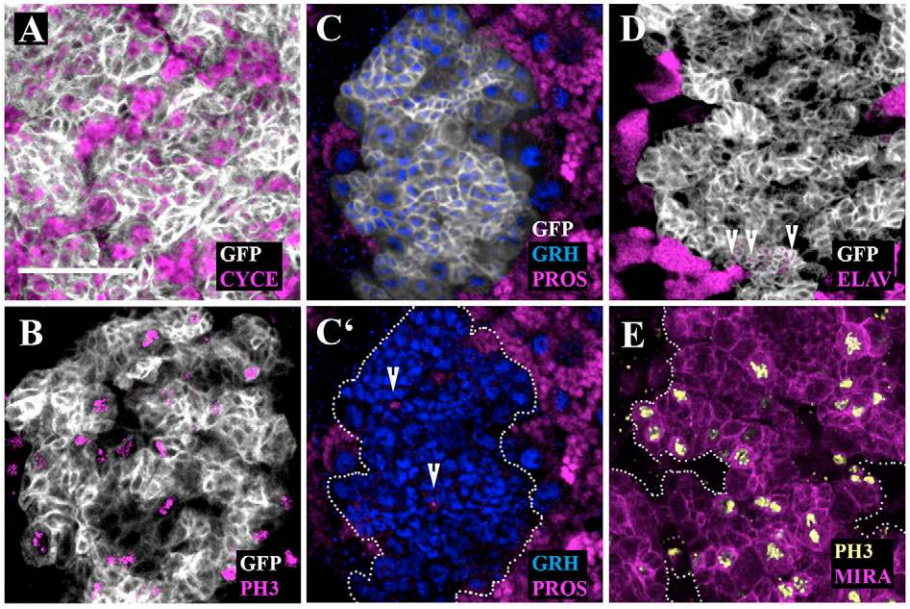

Fig. 4. *brat* mutant clones comprise an excessive number of neural progenitor cells. *brat*^{11} MARCM clones positively labelled with CD8::GFP (white) and immunostained as indicated for each panel. The outline of GFP-labelled cellular masses of mutant clones are indicated with dots when GFP label is omitted for clarity. GFP-labelled mutant clones appear heterogeneous in size. (**A**,**B**) Most cells express cyclin E (A) and numerous cells are engaged in mitosis (B, magenta, E, yellow). (**C-E**) In contrast to heterozygous wild-type tissues that surround clones, the majority of *brat* mutant cells show expression of markers characteristic of neural progenitors: nuclear Grh (C,C′; blue) and cortical Mira (E, magenta). Only very few nuclei express Pros (C′, arrowheads) and Elav (D, arrowheads). This apparent deficit in neural differentiation of *brat* mutant cells is also revealed by the absence of axonal processes. Scale bar, 50 μm; genotype as in Fig. 2.

wondered whether *brat* mutant clones cease proliferation or whether they are able to escape cell cycle stop signals during later stages of development. MARCM *brat*^{11} clones were induced in first instar larvae and immunostained for PH3 in adult brains at 1 day, 2 weeks and 3 weeks after eclosion. Control wild-type clones induced in parallel and examined in the brain of adult flies comprised a limited number of cells that never showed PH3 immunoreactivity (Fig. 5A,B), consistent with the general notion that the adult brain is composed of postmitotic cells. In contrast, *brat* mutant clones appeared dramatically enlarged in size and cell number in the adult brain (Fig. 5C). Moreover, a large number of mutant cells displayed PH3 immunoreactivity even in 3-week-old adult flies, suggesting that these mutant cells were still mitotically active (Fig. 5D). These data indicate that loss of larval *brat* function results in mutant cells that are unable to respond to cell cycle termination signals during metamorphosis.

pros mutant clones phenocopy *brat* mutant clones in the larval central brain

The features of *brat* mutant cells reminded us of the CNS phenotype observed in *pros* mutant embryos. During embryonic CNS development, Pros is required for both cell fate specification and proliferation control of neural progenitor cells. In the absence of Pros function, differentiation genes are not activated and progenitor cell-specific genes are not repressed (reviewed by Lu et al., 2000). Loss of Pros function results in continued mitotic activity that correlates with de-repressed, ectopic transcription of cell cycle genes (Li and Vaessin, 2000). This prompted us to investigate whether loss of nuclear Pros expression in *brat* mutant clones could be causally related to the overproliferation phenotype observed.

We therefore generated wild-type MARCM clones and clones mutant for the loss-of-function allele *pros*^{17}. When assayed in third instar larvae, nuclear β-gal or GFP-labelled *pros*^{17} clones appeared to have increased in size and be populating large areas of the central

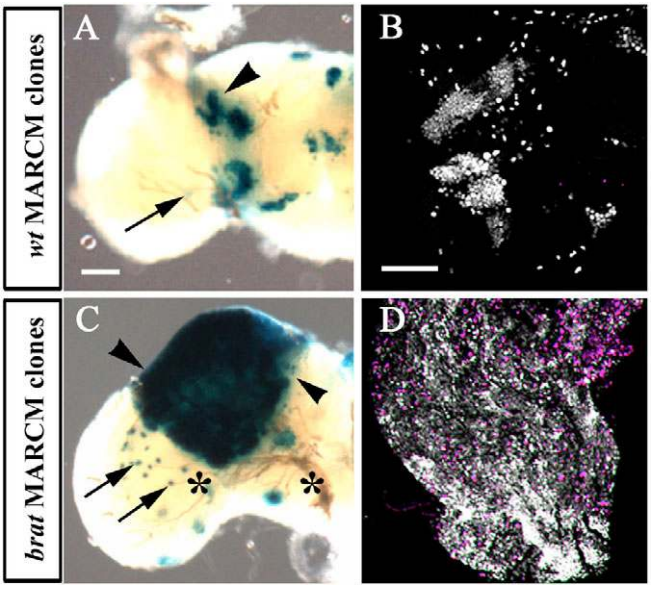

Fig. 5. larval *brat* mutant central brain clones continue to proliferate into adulthood. (**A-D**) Dissected whole-mount 3-week-old adult brains showing MARCM clones which had been induced in early first instar larvae. (A) X-gal detection of nuclear *lacZ* marker (blue) reveals typical sizes of wild-type MARCM clones in central brain (arrowhead) and optic lobe (arrow). (B) Close up view of wild-type clones in central brain immunostained with anti-β-galactosidase (nuclei, white). Wild-type clones lack PH3 immunoreactivity (magenta) consistent with proliferation arrest during puparium formation and metamorphosis. (C) X-gal labelled *brat*^{11} MARCM clones in central brain (arrowheads) are dramatically enlarged in size, whereas mutant clones in optic lobe (arrows) appear wild-type-like. [The brown axon-like structures on the specimen (asterisks) are the remains of the adult head cuticule.] (D) Double-immunolabelling of nuclear β-gal (white) and PH3 (magenta) reveals numerous cells of the enormously enlarged *brat* mutant clones mitotically active even 3 weeks after adult eclosion (compare with B). Scale bars, 50 μm; genotypes as in Fig. 2.

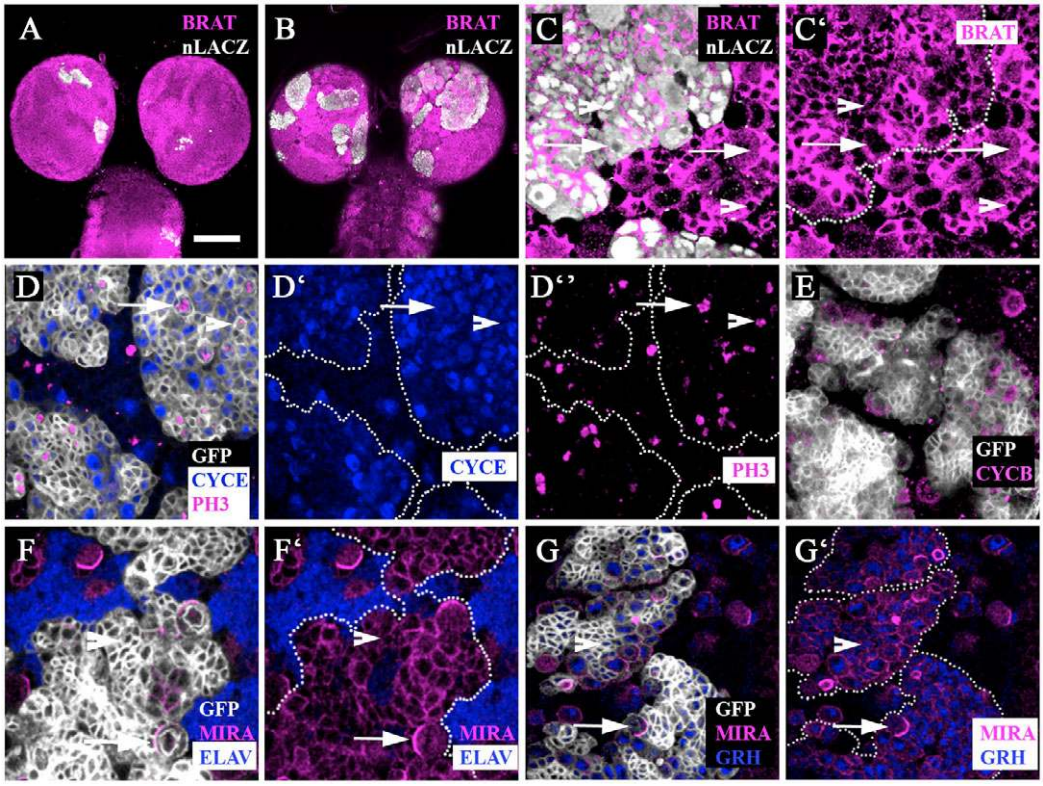

Fig. 6. *Pros* mutant clones phenocopy *brat* mutant clones in the larval central brain. Wild type (**A**) and *pros*^{17} MARCM clones (**B-G′**) labelled with nuclear *lacZ* (A-C, white) or CD8::GFP (D,E,F,G, white) and immunostained as indicated for each panel. *pros*^{17} clones in central brain are enlarged and can cover most of the brain hemisphere (compare B with A) with multiple *pros* mutant clones occasionally merged into a labelled cell mass. (C-G′) Close up views of labelled mutant cells reveal the presence of pleiomorphic cell types including large neuroblast-like cells (arrows) and many smaller cells (arrowheads). Brat expression is ubiquitous in larval CNS (A,B) and detected at comparable levels in cytoplasm of all mutant *pros* cells labelled with nuclear *lacZ*, or in heterozygous wild-type cells that surround labelled mutant cells (C,C′). Many *pros* mutant cells dispersed throughout clones are engaged in mitosis as indicated by PH3 immunoreactivity (D,D″; magenta) and most cells express CycE (D,D′; blue) and CycB (E, magenta), irrespective of their size and location within clones. Only a few nuclei are positive for the postmitotic marker Elav (F,F′; blue), whereas most cell express Mira at the cortex (F-G′; magenta) and Grh in nuclei (G,G′; blue). Cortical expression of Mira is uniform in vast majority of small cells (F-G′, arrowheads), whereas polarized Mira forming crescents can be observed in large neuroblast-like cells (F-G′, arrows). Scale bar, 100 μm (A,B) or 20 μm (C-G). Genotypes: (A) *hsFLP/+; UAS-mCD8::GFP*^{LL5}*, UAS-nlslacZ*^{20b}*/tub-Gal4; FRT82B/FRT82B, tubP-GAL80*^{LL10}; (B-G′) *hsFLP/+; UAS-mCD8::GFP*^{LL5}*, UAS-nlslacZ*^{20b}*/tub-Gal4; FRT82B, pros*^{17}*/FRT82B, tubP-GAL80*^{LL10}.

brain (Fig. 6B) when compared to wild-type control clones (Fig. 6A). The majority of *pros* mutant central brain clones were five to ten times larger than wild-type control clones (n>100). Thus, less than 5% of *pros* mutant clones comprised less than 100 cells, whereas more than 90% of these clones comprised 200-1000 cells. Occasionally we also observed brain hemispheres in which the central brain was almost entirely labelled with nuclear β-gal or GFP, suggesting that multiple *pros* mutant clones had already merged to an indistinguishable labelled cell mass. Close inspection of such a nuclear β-gal-labelled cell mass revealed the presence of numerous pleiomorphic cells including large neuroblast-like cells (Fig. 6C).

In order to correlate Pros expression and function to those of Brat, we carried out anti-Brat immunostaining on third instar larval CNS consisting of either wild-type or *pros* mutant central brain clones (Fig. 6A,B). In both cases, we observed cytoplasmic Brat immunolabelling in all cells of the larval CNS (Fig. 6A,B), regardless of their size and morphology (Fig. 6C,C′). These data suggest that Brat is ubiquitously expressed in the developing wild-type CNS consistent with earlier reports on Brat RNA in situ hybridization and enhancer trap expression studies (Arama et al., 2000). Importantly, we did not observe any difference in anti-Brat immunoreactivity between GFP-labelled *pros* mutant cells and surrounding wild-type heterozygous cells (Fig. 6C,C′). These data suggest that Brat expression is unaffected in larval central brain *pros* mutant clones.

Next, we utilized the molecular markers used to characterize wild-type and *brat* mutant lineages to further analyze *pros* mutant clones. Almost all cells in the clones were found to express CycE (Fig. 6D,D′), CycB (Fig. 6E), and numerous cells displayed PH3 immunoreactivity (Fig. 6D″). Co-labelling with PH3 and CycE showed that CycE is present at significant levels in most mitotic cells, regardless of morphology, size or position within these clones (Fig. 6D′,D″). GFP-labelled *pros* mutant clones did not show any cellular extensions comparable to axon fascicles, suggesting an invariable lack of axonal processes. Moreover, *pros* mutant clones lacked Elav immunoreactivity (Fig. 6F,F′), suggesting the lack of differentiated ganglion cells. By contrast, most *pros* mutant cells showed nuclear Grh (Fig. 6G,G′) and cortical Mira (Fig. 6F-G′). As for wild-type neuroblasts, few large cells scattered at the surface of clones showed polarized Mira distribution in a cortical crescent (Fig. 6F′,G′, arrows), suggesting the presence of several asymmetrically dividing neuroblasts. However, the vast majority of *pros* mutant cells

showed uniform cortical distribution of Mira (Fig. 6F′,G′). These findings indicate that *pros* mutant clones phenocopy larval central brain *brat* mutant clones.

pros can promote cell cycle exit and differentiation of *brat* mutant cells

The remarkable similarities between *brat* and *pros* mutant clones suggested that both genes might act in the same pathway regulating proliferation in the larval central brain. Hence, we used MARCM to express full-length wild-type *pros* specifically in *brat* mutant clones. As a control we tested the ability of a full length wild-type *brat* cDNA (Sonoda and Wharton, 2001) to rescue the *brat* mutant brain phenotype. Targeted expression of wild-type *brat* in *brat* mutant clones (n>50) resulted in a significant reduction of clone size in the central brain of third instar larvae (Fig. 7A-B′). Thus, more than 90% of late third instar central brain clones comprised <100 cells, whereas less than 10% of these clones comprised 100-500 cells. We frequently observed that individual clones merged to form a nest of GFP-labelled cells (Fig. 7A,B), however clones were still distinguishable because only a few superficially located cells showed nuclear Grh (Fig. 7A-B′) and cortical Mira (data not shown). Moreover, most cells within clones expressed Elav (Fig. 7A,A′) and Pros (Fig. 7B,B′) in their nuclei and they formed axonal processes contributing to individual fibre tracts (Fig. 7A,B), indicating the presence and proper differentiation of postmitotic ganglion cells. These data suggest that UAS-driven expression of the *brat* transgene in *brat* mutant clones results in clones that are comparable in size, number and marker gene expression to wild-type controls. In addition, even when examined in the adult brain, these clones appeared similar to wild-type control clones and lacked PH3 staining (data not shown).

Targeted expression of wild-type *pros* in *brat* mutant clones (n>50) resulted in a very similar phenotype (Fig. 7C-D′). More than 90% of late third instar central brain clones comprised <100 cells, whereas less than 10% of these clones comprised 100-500 cells. Similar to the *brat* rescue, a significant decrease in mitotic activity occurred, as exemplified by clone size and by PH3-immunoreactivity restricted to a few large cells and to a limited number of smaller associated cells, both of which expressed cortical Mira and nuclear Grh (Fig. 7C-D′). The presence and proper differentiation of postmitotic ganglion cells could be assessed by the detection of Pros (Fig. 7D,D′) and Elav (not shown) in the vast majority of cells within the clones. Moreover, most cells formed axonal processes assembled in wild-type-like fibre tracts (Fig. 7C,D). Thus, as for *brat*, targeted expression of *pros* in *brat* mutant clones results in clones that are comparable to wild-type lineages in size, number, and marker gene expression. These results demonstrate that *pros* can promote cell cycle exit and differentiation of *brat* mutant cells in a wild-type-like pattern, which in turn abrogates central brain tumour formation.

DISCUSSION

brat is cell-autonomously required for timely cell cycle exit in the larval central brain

Previous studies suggested that *brat* loss-of-function mutants lead to massive cellular overgrowth and tumour formation in larval optic lobes of *Drosophila*. These studies also indicated an embryonic requirement for *brat* to suppress tumour formation (Kurzik-Dumke et al., 1992; Gateff et al., 1993; Woodhouse et al., 1998; Arama et al., 2000). By contrast, our analysis showed that the *brat* overproliferation phenotype is due to loss of proliferation control in the larval central brain; the optic lobes initially appear wild-type-like but subsequently are overgrown by neoplastic central brain *brat* mutant tissue. This conclusion is further supported by MARCM clonal analysis which demonstrated that loss of *brat* function causes overproliferation in the larval central brain only.

Our in vivo mosaic analysis reveals a cell-autonomous, larval requirement for *brat* to limit cell proliferation in the brain. Although *brat* is expressed in all parts of the nervous system both in the embryo (Arama et al., 2000) and larva (our study, Fig. 6A-C),

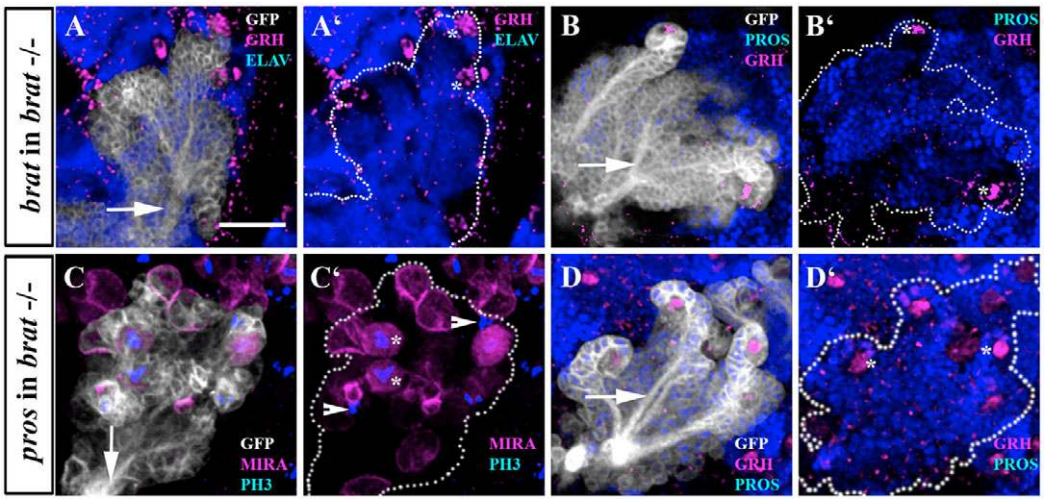

Fig. 7. *pros* can promote cell cycle exit and differentiation of *brat* mutant cells. Targeted expression of UAS-*brat* (**A**,**B**) or UAS-*pros* (**C**,**D**) in *brat*^{11} mutant clones restores wild type-like features of larval central brain lineages. Clones labelled with CD8::GFP (white) were immunostained in late third instar larvae as indicated for each panel. Outline of clones is indicated with dots when GFP label is omitted for clarity. Clones display a limited number of neuroblast-like cells (asterisks) that specifically stain for Grh (A,B,D) or Mira (C). Mitosis is restricted to large nuclei (C,C′; asterisks) or to smaller, closely associated GMC-like cells (C,C′; arrowhead). Most cells in clones project axons contributing to fibre tracts (A-D; arrows) and show nuclear Elav (A,A′) as well as nuclear Pros (B,B′,D,D′). Scale bar, 40 μm. Genotypes: (A,B) *hsFLP/+; FRT40A, brat*^{11}*, UAS-mCD8::GFP*^{LL5}*, UAS-nlslacZ*^{20b}*/FRT40A, tubP-GAL80*^{LL10}*; UAS-brat*^{FL1B}*/tubP-GAL4*^{LL7}. (C,D) *hsFLP/+; FRT40A, brat*^{11}*, UAS-mCD8::GFP*^{LL5}*, UAS-nlslacZ*^{20b}*/FRT40A, tubP-GAL80*^{LL10}*; UAS-pros*$^{L(wt)9D}$*/tubP-GAL4*^{LL7}.

induction of *brat* mutant clones in the first larval instar is sufficient to cause massive overproliferation in the central brain but not the ventral ganglia. This may suggest that either unknown compensatory mechanisms actively suppress a *brat* mutant phenotype in the larval ventral ganglia, or that this reflects region-specific differences in cell cycle control. Indeed, transcriptional activity of the mitotic regulator *string/Cdc25* is regulated by a plethora of cis-acting elements, most of which are devoted to differential control of cell proliferation during embryonic and larval neurogenesis (Lehmann et al., 1999).

During postembryonic neurogenesis, intense proliferation takes place in the brain (Truman and Bate, 1988; Ito and Hotta, 1992). Our analysis shows that central brain *brat* mutant clones display sustained cell cycle marker expression, indicating that mutant cells are unable to withdraw from the cell cycle. This is further supported by the presence of enormous *brat* mutant clones with pronounced proliferative activity even in 3-week-old adult brains, an observation that contrasts with the postmitotic adult wild-type brain. Previous studies have shown that cessation of proliferation in the developing *Drosophila* brain occurs during metamorphosis (Ito and Hotta, 1992), although the underlying genetic mechanisms are currently unknown. The elevated and aberrant cell cycle activity of central brain *brat* mutant cells suggests that these cells are either able to escape or that they lack cell cycle termination signals (Peterson et al., 2002; Bello et al., 2003).

brat negatively regulates progenitor cell proliferation by acting on *pros*

Our mosaic analysis demonstrates that enlarged *brat* mutant clones comprise cells that display sustained expression of neural progenitor cell markers, and simultaneously lack marker gene expression specific for differentiating ganglion cells. Indeed, lack of axonal processes suggests that *brat* mutant clones comprise an excessive number of mutant cells that are unable to exit the cell cycle and hence do not differentiate into ganglion cells but rather continue to proliferate. These data indicate that *brat* mutation impairs proliferation control of neural progenitor cells, namely either neuroblasts and GMCs or only one of these progenitors, since in the wild-type central brain only these two cell types are actively engaged in the cell cycle. Based on our analysis we cannot distinguish unambiguously between the two possibilities and the underlying mechanisms. We do, however, exclude the possibility that differentiating ganglion cells de-differentiate due to *brat* mutation, because we consistently observed lack of differentiation right after clone induction and also at any later stages of mutant clone development. This was especially exemplified by the lack of nuclear Pros expression, which in the wild type is unambiguously detectable in differentiating progeny of larval neuroblast lineages, namely GMCs as well as ganglion cells (see Fig. 3) (see also Ceron et al., 2001; Akong et al., 2002).

Moreover, our loss-of-function analysis indicates that *brat* mutant MARCM clones lack Pros and also phenocopy *pros* mutant clones. Thus, enlarged *pros* mutant clones consist of cells that are devoid of Elav expression, that lack axonal processes but display sustained expression of Grh and Mira as well as cell cycle markers such as CycE, CycB and PH3. These data suggest that mutant clones are essentially devoid of terminally differentiating postmitotic ganglion cells, indicating that Pros functions like Brat in terminating neural progenitor cell proliferation and inducing ganglion cell differentiation. In the embryonic CNS, Pros functions to terminate cell proliferation by repression of cell-cycle activators and simultaneously to induce a differentiation program, effectively coupling the two events. This Pros function appears to be warranted by its localization in the basal cortex of asymmetrically dividing neuroblasts and hence its distribution to only one daughter cell, the GMC. Upon completion of mitosis, Pros translocates from cytoplasm into the nucleus where it executes its transcriptional program ensuring both terminal division of the GMC and cell differentiation of its progeny (for a review, see Prokopenko and Chia, 2005). In the larval CNS we observe nuclear localisation of Pros in GMCs and ganglion cells but not in the neuroblast, suggesting that Pros has comparable functional features in larval central brain neurogenesis.

In addition, our results provide evidence that Pros acts downstream of Brat in neural proliferation control. The following points support this notion: (1) *brat* mutant clones lack nuclear Pros; (2) *brat* and *pros* mutant clones are indistinguishable both at the morphological and at the molecular level; (3) Brat expression is unaltered in *pros* mutant clones, which together with point no. 1 strongly suggests that Brat is epistatic over Pros; and (4) trans-activation of wild-type *pros* in *brat* mutant clones is sufficient to promote both cell cycle exit and differentiation. Our experiments, however, do not provide any evidence about the direct or indirect nature of their interaction. Since overexpressed Pros is detected specifically in *brat* mutant clones in a wild-type-like pattern (Fig. 7D′), we exclude the possibility that *brat* acts as a translational repressor of *Pros*, comparable to its role in *hunchback* repression during embryonic abdominal segmentation (Sonoda and Wharton, 2001). In addition, *brat* mutation apparently does not affect *pros* transcription, since *pros* RNA in situ hybridization in zygotic *brat* mutants produced a pattern indistinguishable from wild-type controls (data not shown). Thus, Brat and Pros may act indirectly in the same pathway, regulating progenitor cell proliferation control in the brain. Alternatively, Brat may act in a process required to cargo Pros, comparable to the function of its mammalian homolog BERP (Yan et al., 2005).

Somatic mutation of *brat* and *pros* can cause clonally derived brain tumours

Our in vivo mosaic analysis demonstrates that a single mutation in either *brat* or *pros* is sufficient to cause brain tumour formation in a cell-autonomous manner, suggesting that indefinite proliferation of *brat* and *pros* mutant cells is a cell intrinsic property (Caussinus and Gonzalez, 2005). GFP-labelled MARCM cells each derive from a common precursor cell, implying that *brat* and *pros* mutant cells all descend from individual tumour cells of origin and hence lead to brain tumour formation in a clonally related manner. Moreover, our data indicate that *pros* and *brat* mutant clones in the larval central brain are composed of an excessive number of mutant progenitor cells that are unable to differentiate into ganglion cells but rather continue to proliferate (summarized in Fig. 8). In this sense our results provide in vivo support for the notion that the initiating event in the formation of a malignant tumour is an error in the process of normal differentiation (Harris, 2005).

In addition, the unlimited capacity to generate undifferentiated, proliferating progeny suggests that cells mutant for *brat* or *pros* retain self-renewing capacities. In human, brain cancers are thought to arise either from normal stem cells or from progenitor cells in which self-renewal pathways have become activated (reviewed in Al-Hajj and Clarke, 2004; Oliver and Wechsler-Reya, 2004), however the underlying mechanisms are elusive. Our results in *Drosophila* may therefore provide a rationale and genetic model for the origin of brain cancer stem cells. Although parallels to human tumour formation are speculative, it is noteworthy that *TRIM3,* a human homolog of *brat* is located on chromosome 11p15 (El-Husseini et al., 2001), a region frequently deleted in brain tumours (Fults et al., 1992; Sonoda et al., 1995; Schiebe et al., 2001). Moreover, functional studies have shown that the *pros* homologue

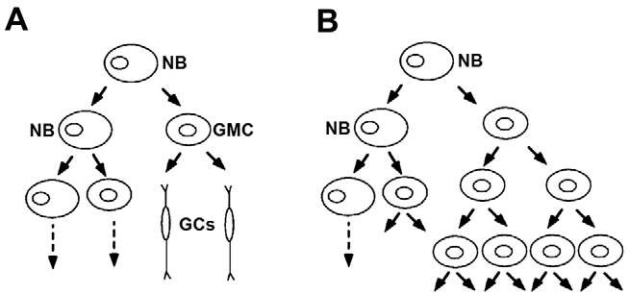

Fig. 8. Neural lineage formation in the larval central brain of wild-type, *brat* and *pros* mutant clones. (**A**) In wild-type *Drosophila*, neural progenitor cells are required for lineage formation: neuroblasts (NB) divide asymmetrically to self-renew and to produce a series of ganglion mother cells (GMC); GMCs instead differentiate by undergoing a single terminal division that produces two postmitotic ganglion cells (GCs). GCs send out axons contributing to fibre tracts. (**B**) Somatic mutation of the tumour suppressor *brat*, and loss of function of the cell fate determinant *pros* impede differentiation of progenitor cells into GCs. Instead, these mutant cells retain progenitor cell-like characteristics and indefinitely self-renew, thereby generating clonally derived brain tumours. Targeted misexpression of either *brat* or *pros* in *brat* mutant cells restores differentiation which abrogates brain tumour formation.

Prox1 regulates proliferation and differentiation of neural progenitor cells in the mammalian retina (Dyer et al., 2003). These data may indicate that *brat* and *pros* function in cell differentiation and tumour suppression in an evolutionarily conserved manner.

Note added in proof

While this manuscript was under review, Betschinger et al. (Betschinger et al., 2006) and Lee et al. (Lee et al., 2006) reported comparable findings on the function of *brat* in larval central brain tumour suppression.

We thank Y.-A. Barde, A. Merlo, K.-F. Fischbach, M. C. Ionescu, and J.-L. Boulay for critical review; T. Loop and L. Kammermeier for initial contributions; U. Stiefel for technical assistance; and M. Akam, S. J. Bray, C. Q. Doe, B. Edgar, D. Frank, P. Overton, H. Richardson, R. P. Wharton, the Bloomington Stock Center and the Developmental Studies Hybridoma Bank for strains and reagents. This work was supported by grants from the Swiss NSF (to H.R.), the Roche Research Foundation, Oncosuisse, and the Krebsliga beider Basel (to F.H.).

References

Akong, K., McCartney, B. M. and Peifer, M. (2002). Drosophila APC2 and APC1 have overlapping roles in the larval brain despite their distinct intracellular localizations. *Dev. Biol.* **250**, 71-90.
Al-Hajj, M. and Clarke, M. F. (2004). Self-renewal and solid tumor stem cells. *Oncogene* **23**, 7274-7282.
Almeida, M. S. and Bray, S. J. (2005). Regulation of post-embryonic neuroblasts by *Drosophila* Grainyhead. *Mech. Dev.* **122**, 1282-1293.
Arama, E., Dickman, D., Kinchie, Z., Shearn, A. and Lev, Z. (2000). Mutations in the beta-propeller domain of the *Drosophila brain tumor* (*brat*) protein induce neoplasm in the larval brain. *Oncogene* **19**, 3706-3716.
Bello, B. C., Hirth, F. and Gould, A. P. (2003). A pulse of the Drosophila Hox protein Abdominal-A schedules the end of neural proliferation via neuroblast apoptosis. *Neuron* **37**, 209-219.
Betschinger, J., Mechtler, K. and Knoblich, J. A. (2006). Asymmetric segregation of the tumor suppressor brat regulates self-renewal in Drosophila neural stem cells. *Cell* **124**, 1241-1253.
Campos-Ortega, J. A. (1997). Neurogenesis in Drosophila: a historical perspective and some prospects. *Perspect. Dev. Neurobiol.* **4**, 267-271.
Campos-Ortega, J. and Hartenstein, V. (1997). *The Embryonic Development of Drosophila melanogaster*. Heidelberg: Springer-Verlag.
Caussinus, E. and Gonzalez, C. (2005). Induction of tumour growth by altered stem-cell asymmetric division in Drosophila melanogaster. *Nat. Genet.* **37**, 1125-1129.
Cenci, C. and Gould, A. P. (2005). Drosophila Grainyhead specifies late programmes of neural proliferation by regulating the mitotic activity and Hox-dependent apoptosis of neuroblasts. *Development* **132**, 3835-3845.
Ceron, J., Gonzalez, C. and Tejedor, F. J. (2001). Patterns of cell division and expression of asymmetric cell fate determinants in postembryonic neuroblast lineages of Drosophila. *Dev. Biol.* **230**, 125-138.
Dyer, M. A., Livesey, F. J., Cepko, C. L. and Oliver, G. (2003). Prox1 function controls progenitor cell proliferation and horizontal cell genesis in the mammalian retina. *Nat. Genet.* **34**, 53-58.
Edenfeld, G., Pielage, J. and Klambt, C. (2002). Cell lineage specification in the nervous system. *Curr. Opin. Genet. Dev.* **12**, 473-477.
El-Husseini, A. E.-D., Fretier, P. and Vincent, S. R. (2001). Cloning and characterization of a gene (*RFN22*) encoding a novel brain expressed ring finger protein (BERP) that maps to human chromosome 11p15.5. *Genomics* **71**, 363-367.
Frank, D. J., Edgar, B. A. and Roth, M. B. (2002). The *Drosophila melanogaster* gene *brain tumor* negatively regulates cell growth and ribosomal RNA synthesis. *Development* **129**, 399-407.
Fults, D., Petronio, J., Noblett, B. D. and Pedone, C. A. (1992). Chromosome 11p15 deletions in human malignant astrocytomas and primitive neuroectodermal tumours. *Genomics* **14**, 799-801.
Gateff, E., Loffler, T. and Wismar, J. (1993). A temperature-sensitive brain tumor suppressor mutation of Drosophila melanogaster: developmental studies and molecular localization of the gene. *Mech. Dev.* **41**, 15-31.
Harris, H. (2005). A long view of fashions in cancer research. *BioEssays* **27**, 833-838.
Ito, K. and Hotta, Y. (1992). Proliferation pattern of postembryonic neuroblasts in the brain of *Drosophila melanogaster*. *Dev. Biol.* **149**, 134-148.
Kurzik-Dumke, U., Phannavong, B., Gundacker, D. and Gateff, E. (1992). Genetic, cytogenetic and developmental analysis of the Drosophila melanogaster tumor suppressor gene lethal(2)tumorous imaginal discs (l(2)tid). *Differentiation* **51**, 91-104.
Lee, C. Y., Wilkinson, B. D., Siegrist, S. E., Wharton, R. P. and Doe, C. Q. (2006). Brat is a Miranda cargo protein that promotes neuronal differentiation and inhibits neuroblast selfrenewal. *Dev. Cell* **10**, 441-449.
Lee, T. and Luo, L. (1999). Mosaic analysis with a repressible cell marker for studies of gene function in neuronal morphogenesis. *Neuron* **22**, 451-461.
Lee, T. and Luo, L. (2001). Mosaic analysis with a repressible cell marker (MARCM) for Drosophila neural development. *Trends Neurosci.* **24**, 251-254.
Lehman, D. A., Patterson, B., Johnston, L. A., Balzer, T., Britton, J. S., Saint, R. and Edgar, B. A. (1999). Cis-regulatory elements of the mitotic regulator, string/Cdc25. *Development* **126**, 1793-1803.
Li, L. and Vaessin, H. (2000). Pan-neural Prospero terminates cell proliferation during Drosophila neurogenesis. *Genes Dev.* **14**, 147-151.
Loop, T., Leemans, R., Stiefel, U., Hermida, L., Egger, B., Xie, F., Primig, M., Certa, U., Fischbach, K. F., Reichert, H. et al. (2004). Transcriptional signature of an adult brain tumour in Drosophila. *BMC Genomics* **5**, 24.
Lu, B., Jan, L. and Jan, Y. (2000). Control of cell divisions in the nervous system: symmetry and asymmetry. *Annu. Rev. Neurosci.* **23**, 531-556.
Matsuzaki, F., Koizumi, K., Hama, C., Yoshioka, T. and Nabeshima, Y. (1992). Cloning of the *Drosophila prospero* gene and its expression in ganglion mother cells. *Biochem. Biophys. Res. Comm.* **182**, 1326-1332.
Oliver, T. G. and Wechsler-Reya, R. J. (2004). Getting at the root and stem of brain tumours. *Neuron* **42**, 885-888.
Peterson, C., Carney, G. E., Taylor, B. J. and White, K. (2002). reaper is required for neuroblast apoptosis during Drosophila development. *Development* **129**, 1467-1476.
Prokop, A. and Technau, G. M. (1991). The origin of postembryonic neuroblasts in the ventral nerve cord of *Drosophila melanogaster*. *Development* **111**, 79-88.
Prokopenko, S. N. and Chia, W. (2005). When timing is everything: role of cell cycle regulation in asymmetric division. *Semin. Cell Dev. Biol.* **16**, 423-437.
Reddy, G. V. and Rodrigues, V. (1999). Sibling cell fate in the Drosophila adult external sense organ lineage is specified by prospero function, which is regulated by Numb and Notch. *Development* **126**, 2083-2092.
Schiebe, M., Ohneseit, P., Hoffmann, W., Meyermann, R., Rodemann, H. P. and Bamberg, M. (2001). Loss of heterozygositiy at 11p15 and p53 alterations in malignant gliomas. *J. Cancer Res. Clin. Oncol.* **127**, 325-328.
Skeath, J. B. and Thor, S. (2003). Genetic control of Drosophila nerve cord development. *Curr. Opin. Neurobiol.* **13**, 8-15.
Sonoda, Y., Iizuka, M., Yasuda, J., Makino, R., Ono, T., Kayama, T., Yoshimoto, T. and Sekiya, T. (1995). Loss of heterozygosity at 11p15 in malignant glioma. *Cancer Res.* **55**, 2166-2168.
Sonoda, J. and Wharton, R. P. (2001). Drosophila Brain Tumour is a translational repressor. *Genes Dev.* **15**, 762-773.
Technau, G. M., Berger, C. and Urbach, R. (2006). Generation of cell diversity and segmental pattern in the embryonic central nervous system of Drosophila. *Dev. Dyn.* **235**, 861-869.

Truman, J. W. and Bate, M. (1988). Spatial and temporal patterns of neurogenesis in the central nervous system of *Drosophila melanogaster*. *Dev. Biol.* **125**, 145-157.

Truman, J. W., Schuppe, H., Shepherd, D. and Williams, D. W. (2004). Developmental architecture of adult-specific lineages in the ventral CNS of Drosophila. *Development* **131**, 5167-5184.

Uv, A. E., Harrison, E. J. and Bray, S. J. (1997). Tissue-specific splicing and functions of the Drosophila transcription factor Grainyhead. *Mol. Cell. Biol.* **17**, 6727-6735.

White, K. and Kankel, D. R. (1978). Patterns of cell division and cell movement in the formation of the imaginal nervous system of *Drosophila melanogaster*. *Dev. Biol.* **65**, 296-321.

Woodhouse, E., Hersperger, E. and Shearn, A. (1998). Growth, metastasis, and invasiveness of *Drosophila* tumors caused by mutations in specific tumor suppressor genes. *Dev. Genes Evol.* **207**, 542-550.

Yan, Q., Sun, W., Kujala, P., Lotfi, Y., Vida, T. A. and Bean, A. J. (2005). CART: an Hrs/actinin-4/BERP/myosin V protein complex required for efficient receptor recycling. *Mol. Biol. Cell* **16**, 2470-2482.